

Parametric analysis of a glass-micro fibre-reinforced PTFE material, multiband, patch-structure antenna for satellite applications

M. SAMSUZZAMAN*, M. T. ISLAM^a, J. S. MANDEEP^a

Faculty of Engineering and Built Environment, Universiti Kebangsaan Malaysia

^aInstitute of Space Science (ANGKASA), Universiti Kebangsaan Malaysia

This paper presents a fractal, triangular-shaped, multiband, satellite-application antenna created using glass-microfiber-reinforced PTFE material. Different substrate materials are used to determine the performance and characteristics of the proposed antenna design. The radiating patch of the antenna consists of two triangular shapes with two triangular-shaped slots that are connected via a microstrip line and a small slit, while the heptagon ground-plane shape consists of a heptagon slot. The antenna made from the proposed material has attained bandwidths of 45 MHz, 110 MHz, 150 MHz and 230 MHz at centre frequencies of 5.67 GHz, 6.52 GHz, 7.66 GHz and 8.88 GHz, respectively. Experiments have been performed to test the design of the proposed antenna. In addition, the effects of different geometrical parameters on the performance of the antenna have been analysed using a 3D EM solver HFSS (High Frequency Structure Simulator). The physical antenna dimensions are 30 mm x 40 mm x 1.575 mm.

(Received April 16, 2013; accepted September 18, 2013)

Keywords: Composite material, Multiband, Triangular, Satellite, Patch antenna, Slotted

1. Introduction

Presently, the whole world is connected via a satellite communication network. A satellite is usually linked to an earth station by a microwave signal, which is transmitted and received through antennas. The antenna is central to the design and development of satellite communication. Different types of antenna are used in communication satellites. The maturation of antenna technology has been accompanied by cost reductions in substrate materials and manufacturing processes and simplification of design processes via newly developed CAD tools. As a result, current satellite communication applications have been considerably improved by the compact size, lightweight characteristics and low profile of the microstrip antenna.

Mechanical design of microstrip antennas for satellite communication must take into account mechanical conditions (i.e., dimensions, weight, vibrations, acoustics, thermal characteristics, strength, stiffness and deployment shock) and carefully select materials that accommodate these conditions. Although the primary purpose of the substrate material of a microstrip antenna is to provide mechanical support for radiating patch elements, this substrate material plays an important role in microstrip antenna design and production and finished product performance. Particularly in satellite applications, the parameters of the substrate material are key factors that determine antenna performance. In addition to its dielectric constant and dissipation factor, the microwave substrate material has other characteristic properties, including its volume resistivity, surface resistivity, tensile modulus, compressive modulus, water absorption, specific gravity, heat distortion temperature, thermal conductivity and thermal expansion. The selection of material for a

microstrip antenna should be based on cost, insertion loss, thermal stability and dielectric constant, among other considerations [1]. A wireless communication system requires antennas that have large bandwidths and fewer dimensions than have previously existed. Various types of multiband antennas can be made based on the idea of fractal geometry because of proving itself the Sierpinski as an attractive and excellent multiband antenna. Because of the self-similarity of fractal geometry, an antenna possesses multiband and ultra-band characteristics [2, 3]. Different shapes and techniques have been evaluated and found to be appropriate for multiband usage [4-8]. The microstrip triangular patch searches various applications that have many useful MIC components, such as circulators, resonators and filters. The triangular patches have been read practically as well as theoretically [9-13]. They deliver radiation properties similar to those of small-sized rectangular patches. We have attempted to design a triangular fractal antenna that exhibits effective radiation, intact size and multiband properties. Clearly, greater demand has been created due to the rapid growth of wireless communications and the resulting need for electronics (for wireless devices) that can obey different rules and have different standards. Processes for decreasing the size of a microstrip patch antenna are reported widely and include capacitive loading [14], an LC resonator [15] and reactive loading [16]. However, these processes predominantly consider antenna bandwidth or antenna efficiency to decrease antenna size. Alternative processes for constructing multiband microstrip patch antennas have also been disclosed, such as including parasitic elements [17] to create an additional resonant frequency or including more radiating elements that share a similar feed and ground [18, 19]. These processes extend

the physical size of the antenna to produce multiband properties. Thus, there is a trade-off between the number of bands used and the antenna size. The multiband resonance frequency is produced and manipulated by balancing the number of turns of the spiral AMC ground plane [20].

The present study analyses different substrate materials used in a satellite antenna and attempts to achieve multiband characteristics. After analysing different substrate materials, the authors proposed a newly shaped microstrip, which is comprised of two triangular slots and two triangular radiating patches that achieves multiband characteristics and operates at a medium frequency that is appropriate for spacecraft, aircraft and satellite-based communication systems.

Substrate Material

Six different substrate materials, the properties of which are summarised below are used in the simulation studies presented herein.

The FR4 substrate material consists of an epoxy matrix reinforced by woven glass. This composition of epoxy resin and fibre glass varies in thickness and is direction dependent. One of the attractive properties of polymer resin composites is that they can be shaped and reshaped without losing their material properties.[21]. The composition ratio of the material is 60% fibre glass and 40% epoxy resin.

RT/Duroid 5870-filled PTFE composites are designed for exacting strip-line and microstrip circuit applications. The unique filler results in a low density, lightweight material that is beneficial for high-performance, weight-sensitive applications. The very low dielectric constants of such RT/Duroid 5870 laminates are uniform from panel to panel and are constant over a wide frequency range. These materials have been used for airborne antenna systems, lightweight feed networks, military radar systems, missile guidance systems and point-to-point digital radio antennas.

Aluminium oxide is the standard microelectronic substrate material for the vast majority of these applications. Although it has low thermal conductivity, Al₂O₃ has excellent mechanical and electrical properties and is used in DC to High Frequency applications. Aluminium oxide is available as a standard, 96% grade for low cost, general electronics and as a 99.6% grade for higher-frequency applications.

ArlonDiClad laminates are woven fibreglass/PTFE-composite materials that are used as printed circuit-board substrates [22]. Using precise control via the fibreglass/PTFE ratio, DiClad laminates offer a range of choices from the lowest dielectric constant and dissipation factor to a more highly reinforced laminate with better dimensional stability. DiClad laminates are frequently used in filter, coupler and low noise amplifier applications, where dielectric-constant uniformity is critical. They are also used in power dividers and combiners, where low loss is important.

NeltecNX 9240 has superior mechanical and electrical performance, making it the material of choice for low-loss, high-frequency applications, such as wireless communications. This material is specially designed for very low-loss antenna applications. The enhanced N9000 materials reduce passive intermodulation issues in antenna and high-power designs. Benzocyclobutene is frequently used to create photosensitive polymers. BCB-based polymer dielectrics may be spun on or applied to various substrates for use in Micro Electromechanical Systems (MEMS) and microelectronics processing.

2. Antenna design architecture

The geometry and configuration of the proposed antenna is depicted in Fig. 1 a (front view), 1 b (back view) and 1 c (side view). The antenna consists of two triangle slots with two triangular patches that are connected via a microstrip line.

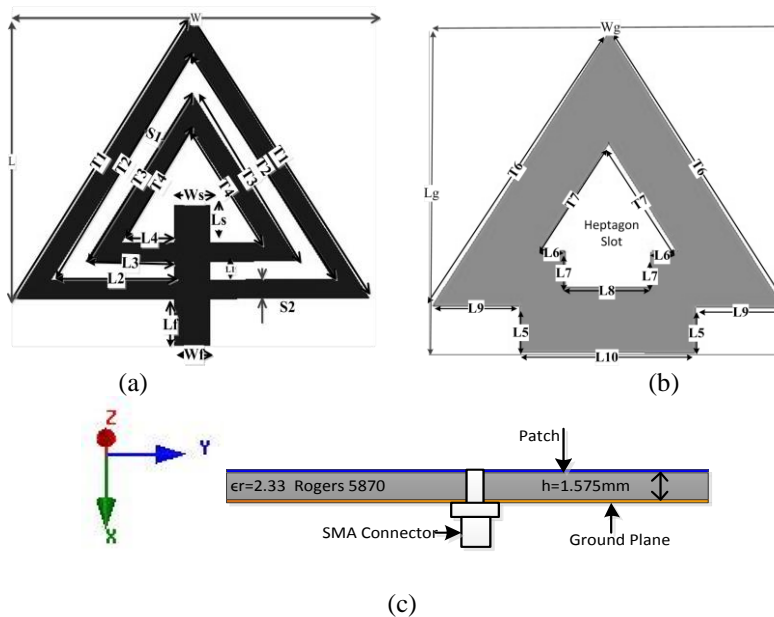


Fig. 1. Proposed antenna geometry a) Top view b) Bottom view c) Side view.

On the other hand, the ground plane has a pentagon shape and a small pentagon-shaped slot etched out from the large one. The slot and tuning stub are printed on the opposite side of a Rogers/RT Duroid 5870 substrate, which has a thickness of 1.575 mm, a low dielectric constant (2.33) and comparatively less tangent loss. The characteristic impedance of the microstrip line is taken as

50 Ω . Fig. 2 represents the impedance of four resonance frequencies using the Smith chart, where VSWR < 2. By properly selecting the slot and tuning stub, a good impedance bandwidth with multiband characteristics is achieved. The optimised antenna parameters are arranged in Table 1.

Table 1. Parameters of the proposed antenna.

Parameter	Value (mm)	Description	Parameter	Value (mm)	Description
L	30	Length of the Patch	S1	2	Slot width
W	40	Width of the Patch	S2	2	Single patch width
Ws	4	Width of the inner I slit	Parameters of Ground Plane		
Ls	4	Length of the inner slit	T6	36.05	First Triangular arm length
Wf	4	Width of the feed	T7	14.42	Slot arm length
Lf	5	Length of the feed	L5	5	
T1	36.05	First equatorial triangular patch arm length	L6	3	
T2	28.84	Second equatorial triangular slot arm length	L7	4	Different arm length
T3	21.63	Third equatorial triangular patch arm length	L8	10	
T4	14.42	Fourth equatorial triangular slot arm length	L9	10	
L1	2	Length of two equatorial triangular patch connecting slit	L10	20	
L2	18	Arm length	W _{Gnd}	40	Width of Ground plane
L3	14		L _{Gnd}	35	Length of ground plane
L4	10				
L5	6				

3. Results and discussions

3.1 Simulated antenna performance

Based on the above optimised design parameters, six substrate materials were studied numerically to investigate the influence of the design parameter on antenna performance. In this analysis, only the substrate material (and dielectric constant) is changed. Figs. 3 and 4 depict the six substrate-material reflection coefficients and average peak gains. The Rogers PTFE-material reflection coefficients and average peak gain is superior to those of all other materials analysed. Tables 2 and 3 show the different parameters values of the proposed antenna shape.

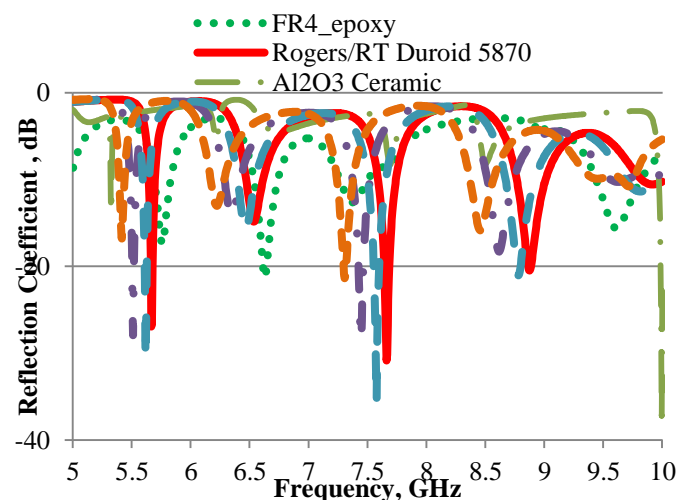


Fig. 2. Different substrate material reflection coefficients of the proposed design.

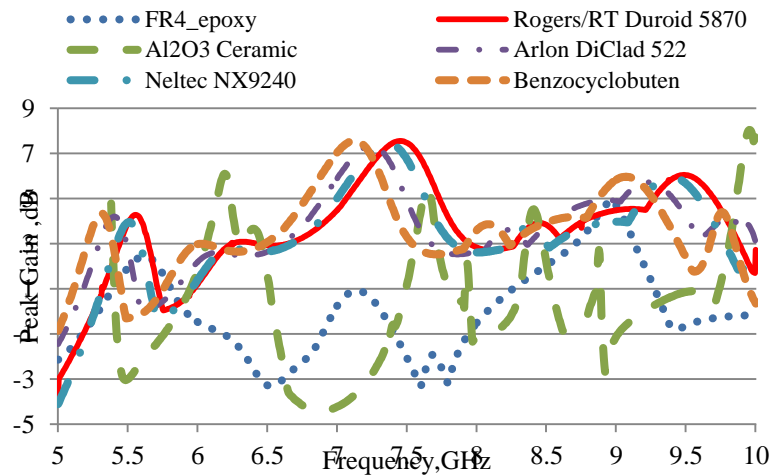


Fig. 3. Peak gain of different substrate material of the proposed design.

Table 2. Different antenna parameters from different material through proposed design.

Substrate Material	Dielectric Constant(ϵ_r)	loss Tangent value(δ)	Resonance Frequency (GHz) & Maximum Return Loss(dB)				Average Peak Gain(dB)				Bandwidth (MHz)			
			fc1	fc2	fc3	fc4	fc1	fc2	fc3	fc4	Bw1	Bw2	Bw3	Bw4
FR4_epoxy	4.6	.02	5.75 & -17.43	6.63 & -21.2	7.37 & -12.63	9.61 & -15.61	1.56	-	-	-	135	200	235	380
Rogers RT/duroid	2.33	.0012	5.67 & -26.52	6.52 & -14.8	7.66 & -30.85	8.88 & -20.4	2.20	2.91	5.96	4.30	50	140	145	245
Al2O3 ceramic	9.8	0	-	-	-	9.99 & -20.99	-	-	-	7.53	-	-	-	25
ArlonDiClad	2.5	.0018	5.51 & -27.93	6.34 & -14.38	7.45 & -28.59	8.63 & -17.81	2.34	2.46	5.56	4.40	50	130	140	215
Neltec NY	2.4	.0016	5.61 & -26.71	6.45 & -15.50	7.57 & -35.84	8.79 & -20.63	2.63	2.17	5.75	3.75	50	140	150	245
Benzocyclobuten	2.6	0	5.41 & -16.67	6.22 & -13.05	7.30 & -21.35	8.46 & -21.35	2.06	2.68	6	3.84	40	110	135	200

Table 3. Different antenna parameters with different substrate material.

Material	Resonance Frequency	Max U (W/sr)	Peak Directivity	Peak Gain	Peak Realized Gain	Radiated Power	Accepted Power	Incident Power	Radiation Efficiency	Front to Back Ratio
FR4 epoxy	5.67	0.00103	3.931	1.703	1.530	0.0033	0.0076	0.0084	0.433	236.126
	6.52	0.00027	1.261	0.467	0.407	0.0027	0.0073	0.0084	0.370	9.484
	7.66	0.00036	1.063	0.617	0.534	0.0042	0.0073	0.0084	0.580	49.480
	8.88	0.00116	4.055	2.734	1.721	0.0036	0.0053	0.0084	0.674	100.122
Rogers/RT Duroid 5870	5.67	0.00115	1.980	1.721	1.698	0.0073	0.0084	0.0085	0.869	7.260
	6.52	0.00123	2.019	1.959	1.822	0.0077	0.0079	0.0085	0.971	37.659
	7.66	0.00268	4.089	4.009	3.961	0.0082	0.0084	0.0085	0.980	814.598
	8.88	0.00178	2.786	2.695	2.634	0.0081	0.0083	0.0085	0.967	17.958
Al2O3 Ceramic	5.67	0.00018	0.685	0.676	0.267	0.0033	0.0033	0.0084	0.987	74.667
	6.52	0.00027	1.199	1.208	0.395	0.0028	0.0028	0.0084	1.007	3.314
	7.66	0.00190	3.415	3.457	2.828	0.0070	0.0069	0.0084	1.012	64.310
	8.88	0.00068	1.535	1.793	1.019	0.0056	0.0048	0.0084	1.168	7.885
ArlonDiClad 522	5.67	0.00025	1.020	0.900	0.378	0.0031	0.0035	0.0084	0.882	57.575
	6.52	0.00098	1.923	1.858	1.459	0.0064	0.0066	0.0084	0.967	39.307
	7.66	0.00092	2.127	2.048	1.369	0.0054	0.0056	0.0084	0.962	506.158
	8.88	0.00148	2.782	2.653	2.200	0.0067	0.0070	0.0084	0.954	13.780
Neltec NX9240	5.67	0.00061	1.351	1.165	0.911	0.0057	0.0066	0.0084	0.863	6.032
	6.52	0.00115	1.909	1.846	1.713	0.0076	0.0078	0.0084	0.967	39.379
	7.66	0.00177	2.987	2.892	2.640	0.0075	0.0077	0.0084	0.968	3485.500
	8.88	0.00158	2.598	2.454	2.360	0.0077	0.0081	0.0084	0.944	14.981
Benzocyclobuten	5.67	0.00019	1.096	1.065	0.279	0.0022	0.0022	0.0085	0.971	34.873
	6.52	0.00061	1.351	1.165	0.911	0.0057	0.0066	0.0084	0.863	6.032
	7.66	0.00057	1.805	1.821	0.853	0.0040	0.0040	0.0084	1.009	110.038
	8.88	0.00147	3.201	3.177	2.195	0.0058	0.0058	0.0084	0.992	30.009

The Smith chart of the proposed antenna is shown in Fig. 4, where fc1, fc2, fc3 and fc4 represent four resonance frequencies. The input impedance of these resonance frequencies is approximately 50 Ω, which is denoted by the RX value. For these resonant frequencies, VSWR < 2.

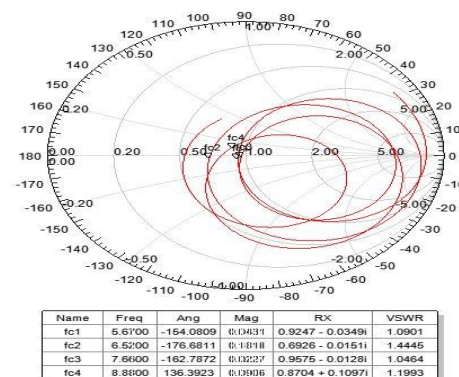


Fig. 4. Smith chart of the proposed antenna.

Fig. 5 illustrates the patch evolution from the conventional triangular-shaped antenna to the propose shape. By cutting different types of slots, the final proposed shaped becomes responsible for multi

resonances. Fig. 6 displays the reflection coefficients of the different patches.

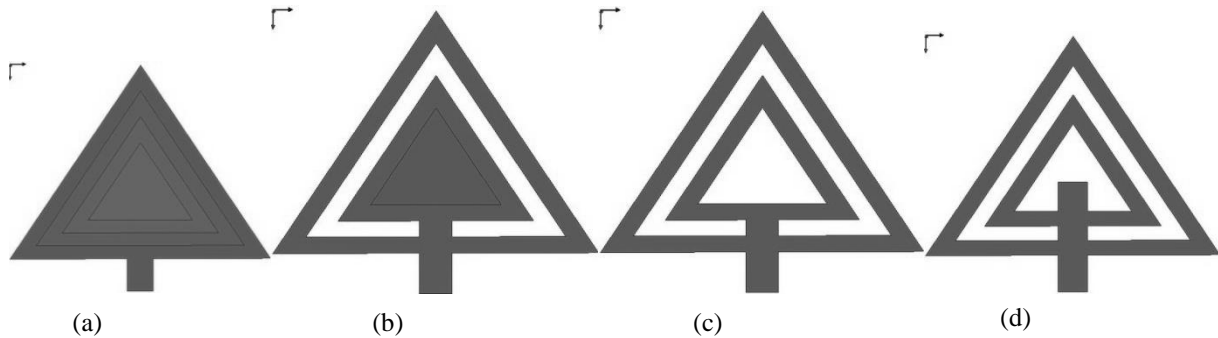


Fig. 5. Evolution from the conventional triangular patch to the proposed patch.

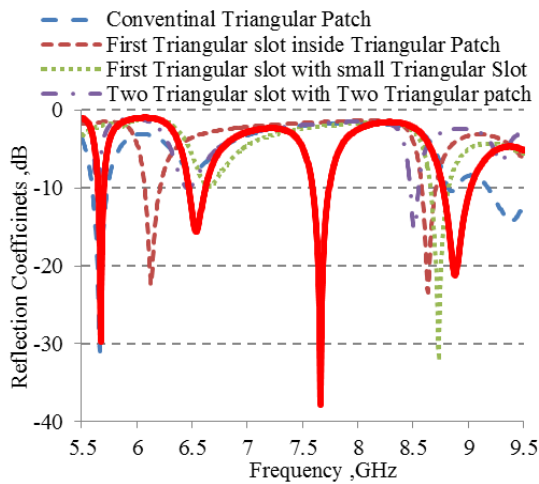


Fig. 6. Simulated reflection coefficient against frequency for different patch shapes.

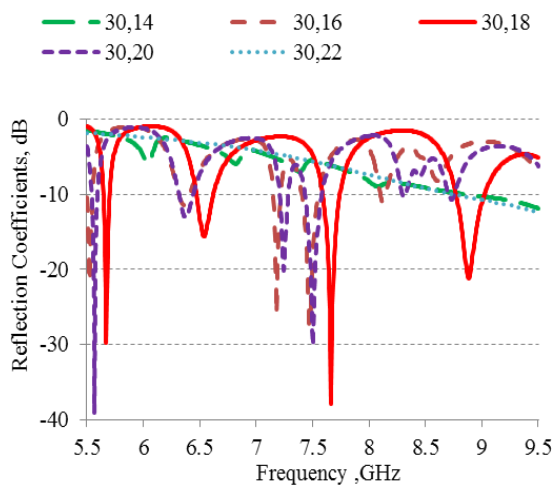


Fig. 7. Simulated return loss for different different feed position.

The different probe feed positions are shown in Fig. 7, where 30, 18 is the position pertaining to optimised antenna performance. Figs. 8 and 9 depict the transmission responses that result from different slit-width (W_s) and slit-length (L_s) values. The slit achieves a good impedance response. The return loss of the proposed antenna is optimal when $W_s = 4$ mm and $L_s = 4$ mm (when all other parameter values (Table 1) remain unchanged). Fig. 10 represents the return loss effect caused by changing the values of feed width (W_f). The optimised feed width is 4 mm (where all other parameter values depicted in table 1 are fixed). The peak gains of the proposed antenna are illustrated in Fig. 11. Average peak gains of 2.20 dB, 2.91 dB, 5.96 dB and 4.30 dB are obtained for different frequency bands.

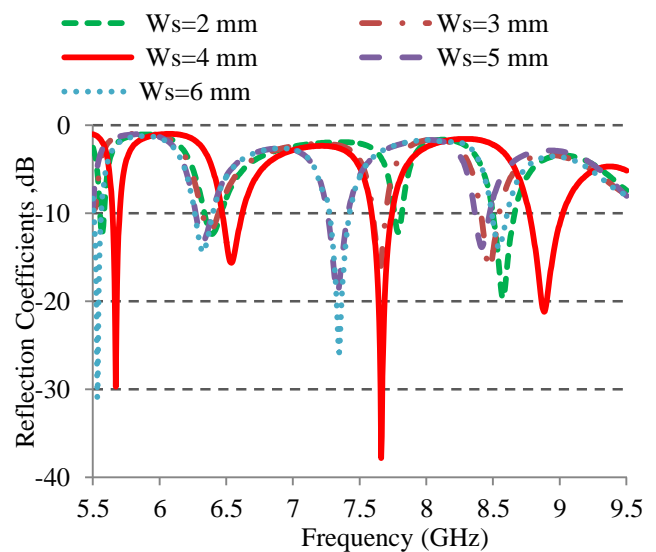


Fig. 8. Simulated reflection coefficient against frequency for different values of W_s .

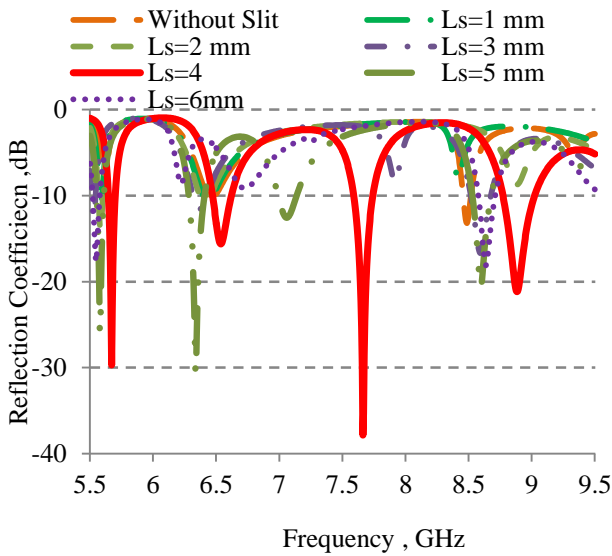


Fig. 9. Simulated reflection coefficient against frequency for different values of Ls.

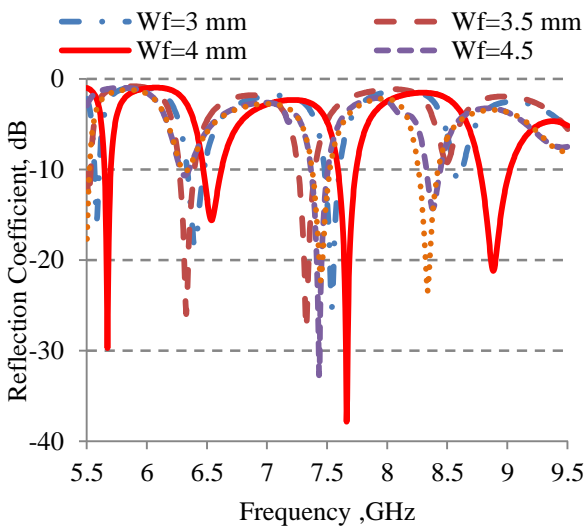


Fig. 11. Simulated peak gain with frequency.

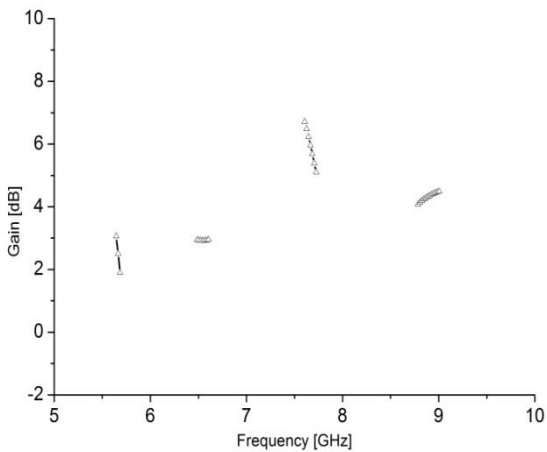


Fig. 10. Simulated return loss for different feed width values of Wf.

The radiation properties in Fig. 12 give an overview of the antenna's behaviour. Fig. 11 is more specific, with the left side displaying the E plane, the right side displaying the H plane, the dotted line representing cross polarisation, and the straight line representing co-polarisation. Cross polarisation is low compared to co-polarisation. The gain pattern of the E plane is nearly omnidirectional, while the H plane is donut shaped.

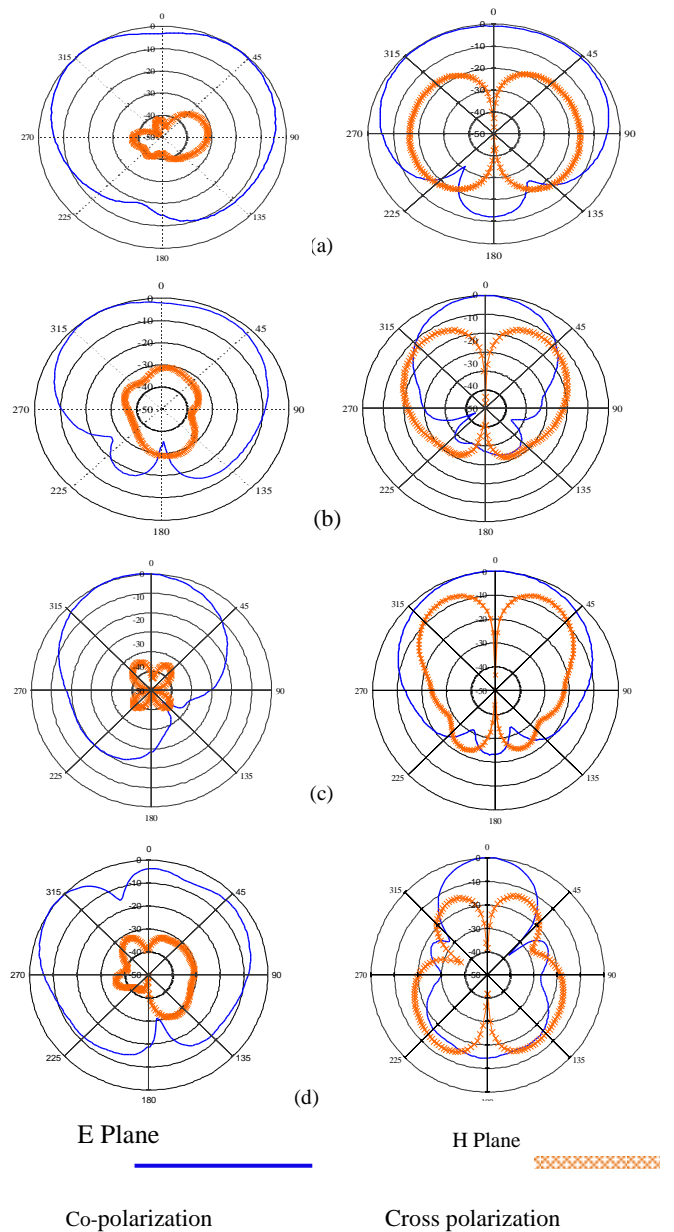


Fig. 12. Radiation pattern of the proposed shape antenna at a) 5.67 GHz b) 6.52 GHz c) 7.66 GHz d) 8.88 GHz.

The radiation efficiencies of the proposed antenna shape at different resonance frequency are shown in Fig. 13. The average radiation efficiencies of the different bands are 85.78%, 97.30%, 98.80% and 95.66% in the achieved particular band.

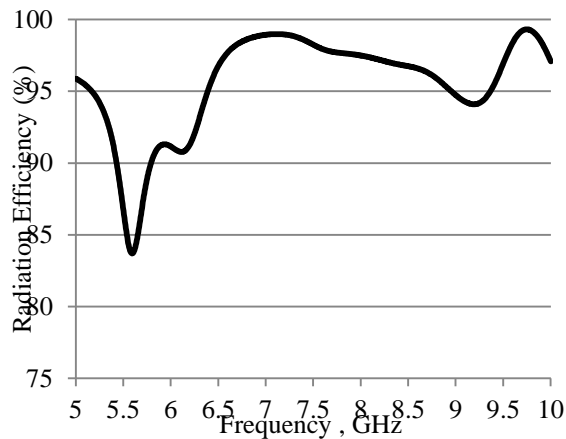


Fig. 13. Radiation efficiency of proposed antenna.

The current distribution of the antenna is given in Fig. 14. The top patch of the antenna is responsible for creating resonances that can be identified by the corresponding current distributions. The blue colour represents low current excitation, and the yellow colour represents high current distribution. The microstrip line is also responsible for good excitation. It is noteworthy that the lower band correlates to a stronger current distribution in most of the radiating area (denoted by green and yellow colours).

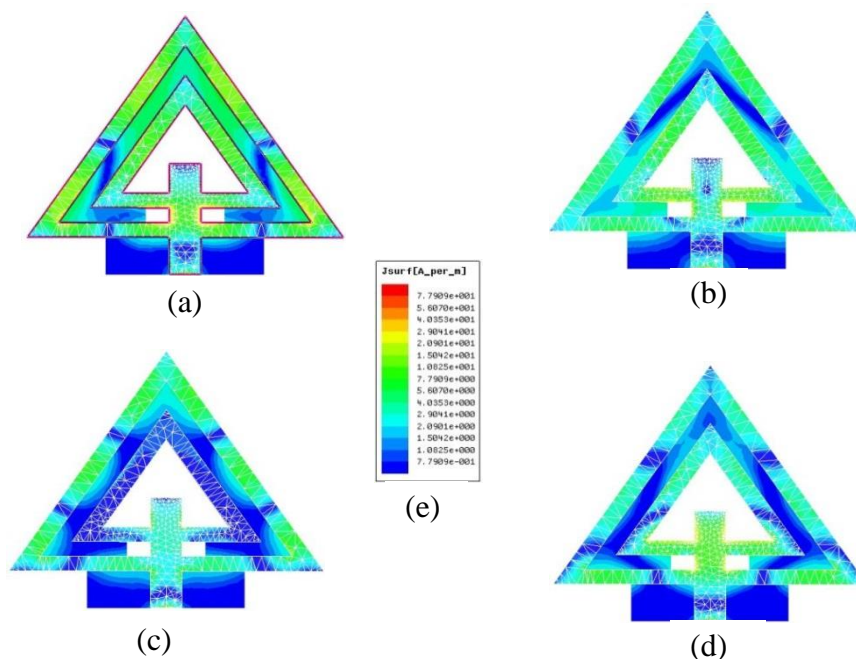


Fig. 14. Current distribution at a) 5.67 GHz b) 6.52 GHz c) 7.66 GHz d) 8.88 GHz.

Table 4 compares the proposed antenna's characteristics with some existing antenna and shows that

the latter antennas have larger sizes, lower gains, or lower efficiencies compared to the proposed antenna.

Table 4. Comparison between the proposed and some existing similar planar structured antennas.

Article	Dimension (mm ²)	Bandwidth (MHz)	Average Gain (dB)
[23]	130×95	642	2.009
[24]	45.46×44.69	1400	N/A
[25]	17.5×10	1250	2
[26]	40×40	951.3	N/A
[27]	32×32	526	N/A
[28]	30.08×45.9	1100	6
Proposed	30×40	45,110,150,230	4.45,3.99,4.17

3.2 Experimental results and discussion

As shown in Fig. 15, an antenna with two triangular slots and a heptagon-slot ground plane has been fabricated on a Rogers RT/Duroid 5870, glass-microfiber-reinforced, PTFE-material substrate (1.575-mm thick) with a relative permittivity (ϵ_r) of 2.33. The measured and simulated reflection coefficients of the proposed antenna are shown in Fig. 16. The 10-dB impedance bandwidths of 45 MHz from 5.67 GHz to 5.715 GHz, 110 MHz from 6.49 to 6.60 GHz, 150 MHz from 7.61 GHz to 7.76 GHz and 230 MHz from 8.81 GHz to 9.04 GHz are clearly evident from the measurements, demonstrating that the measured results are slightly different from the simulated results.

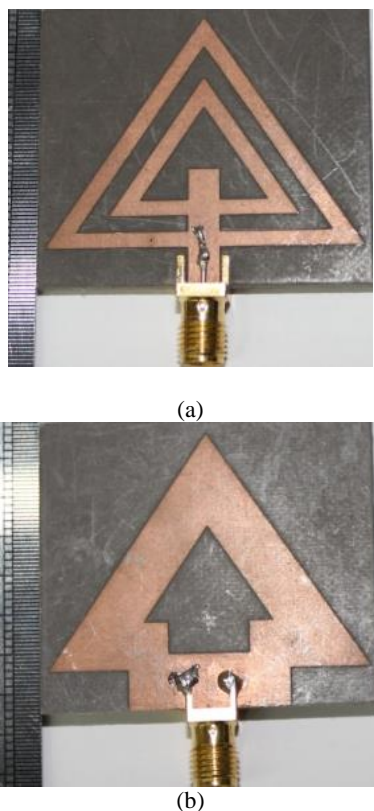


Fig. 15. Prototype of the proposed shape a) Front view
b) Back view.

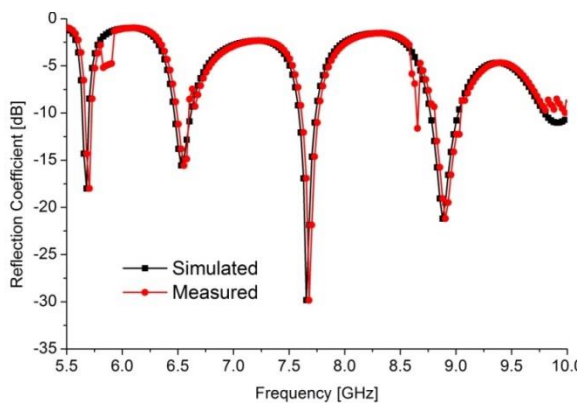


Fig. 16. Measured and simulated return loss with frequency.

4. Conclusion

A new antenna containing a fractal triangular-shaped patch with a heptagon-shaped ground plane has been designed, fabricated and evaluated in this study. The proposed multiband triangular-patch antenna has been analysed using different substrate materials, and the performance characteristics are tabulated in Tables 2 and 3. This analysis demonstrates the superior performance (relative to other reported materials) of the glass-microfiber-reinforced PTFE substrate. The feeding position, the adjusted two-triangular slotted patch and heptagon-slotted ground plane and the antenna dimensions have enabled modification of the acceptable reflection coefficient and the characteristics of the Omni-directional radiation pattern for the expected frequency bands (50 MHz, 140 MHz, 145 MHz and 245 MHz bandwidths). The gain, radiation efficiency, input impedance and current distribution of the proposed antenna have been analysed and discussed. In conclusion, the advancement of glass-microfiber-reinforced PTFE material has fulfilled the specifications required for space application.

Reference

- [1] J. Xia, S. Tan, K. Arichandran, Application of Microstrip Antennas in Small Satellites. Cooperation in Space, Euro-Asian Space Week: where East and West finally meet, Singapore, 23-27 November 1998. Paris: European Space Agency (ESA), ESA-SP 430, 1999. ISBN: 9290927208, p. 459, 1999. 430: p. 459.
- [2] C. Puente-Baliarda, et al., Antennas and Propagation, IEEE Transactions on. 46(4), 517 (1998).
- [3] M. Naghshvarian Jahromi, A. Falahati, R. M. Edwards, IEEE Transactions on, 59(7), 2480 (2011).
- [4] J. Verringer, A. Nafalski, International Journal of Applied Electromagnetics and Mechanics, 13(1), 271 (2002).
- [5] M. H. Ullah, M. T. Islam, J. S. Mandeep, International Journal of Applied Electromagnetics and Mechanics, 41(2), 193 (2013).
- [6] S. Rani, A. P. Singh, International Journal of Applied Electromagnetics and Mechanics.
- [7] S. K. Patel, Y. P. Kosta, International Journal of Applied Electromagnetics and Mechanics, 41(2), 207 (2013).
- [8] Liu, L., et al., International Journal of Applied Electromagnetics and Mechanics, 33(3), 1049 (2010).
- [9] M. Polivka, et al. Multiband patch antenna with perturbation elements generated by genetic algorithm. in Antennas and Propagation, 2006. EuCAP 2006. First European Conference on. 2006. IEEE.
- [10] M. Biswas, M. Dam, Microwave and Optical Technology Letters, 54(11), 2663 (2012).
- [11] R. Garg, S. A. Long, Antennas and Propagation,

- IEEE Transactions on, **36**(4), 570 (1988).
- [12] K. Jhamb, L. Li, K. Rambabu, *Microwaves, Antennas & Propagation, IET.*, **5**(12), 1393 (2011).
- [13] D. Fazal, Q. U. Khan, M .B. Ihsan, *Electronics Letters*, **48**(15), 902 (2012).
- [14] W. Sung-Jung, C. Chi-Hung, T. Jenn-Hwan, 2010 Proceedings of the Fourth European Conference on. 2010.
- [15] D. Yuandan, H. Toyao, T. Itoh, *Antennas and Propagation, IEEE Transactions on*, 2012. **60**(2): p. 772-785.
- [16] M. Deshpande, M. Bailey, *International Symposium, 1997. IEEE., 1997 Digest. 1997. IEEE.*
- [17] Y. J. Cho, S. H. Hwang, S.-O. Park, *Antennas and Wireless Propagation Letters, IEEE*, **4**, 429 (2005).
- [18] P. Ciais, et al., *Electronics Letters*, **40**(15), 920 (2004).
- [19] C. Rowell, A. Mak, C. L. Mak, in *Proc. IEEE APS/URSI/AMEREM Int. Symp.* 2006.
- [20] D. Nashaat, et al. in *Antennas and Propagation Society International Symposium, 2009. APSURSI'09. IEEE. 2009. IEEE.*
- [21] I. Yarovsky, E. Evans, *Polymer.*, **43**(3), 963 (2002).
- [22] M. Ramesh, K. Yip, *Design Inset-Fed Microstrip Patch Antennas. Microwaves & RF*, **42**(12), 64 (2003).
- [23] S.-J. Wu, et al., *IEEE Transactions on*, **58**(2), 593 (2010).
- [24] S. N. Sinha, M. Jain, *Antennas and Wireless Propagation Letters, IEEE*, **6**, 110 (2007).
- [25] M. Samsuzzaman, M. T. Islam, Baharudin Yatim, M. A. Mohd Ali, *Przegląd Elektrotechniczny (Electrical Review)*, 89, 1a (2013).
- [26] F. Y. Zulkifli, F. Narpati, E. T. Rahardjo, *PIERS Online*, **3**(2), 163 (2007).
- [27] N. K. Joshi, A. S. Poonia, P. Choudhary, *International Journal of Computer Applications*, **57**(17), 2012
- [28] K. Aggarwal, A. Garg, *International Journal of Computing and Corporate Research*, **2**(2), 14 (2012).

*Corresponding author: sobuzcse@eng.ukm.my